

FATIGUE CRACK GROWTH PREDICTION OF FIBRE REINFORCED METAL LAMINATES UNDER VARIABLE AMPLITUDE LOADING

S. U. Khan, R. C. Alderliesten, R. Benedictus

Faculty of Aerospace Engineering, Delft University of Technology, The Netherlands

Keywords: *Fatigue crack growth, Fibre metal laminates, variable amplitude loading, crack retardation, GLARE*

Abstract

A recently developed analytical prediction model for constant amplitude loading has been extended to predict fatigue crack growth of Fibre Metal Laminates under variable amplitude loading. Accuracy of the model has been discussed in comparison with the experimental fatigue crack growth data.

1 Introduction

Fibre metal laminates (*FMLs*) consist of alternate layers of uni-directional impregnated fiber lamina and thin metallic sheets adhesively bonded together. *FMLs* are hybrid materials having better mechanical and damage tolerance properties than the individual constituents. *FMLs* have been developed primarily for aircraft structures as a substitute to high strength aluminum alloys.

FMLs have been investigated in the last decades [1–26]. The main advantage of *FMLs* is certainly the very slow and almost constant rate of crack growth under constant amplitude (*CA*) fatigue loading due to the bridging by intact fibers. This bridging effect reduces the effective stress intensity factor resulting in very small interaction effects under variable amplitude (*VA*) loading. Due to this fact, fatigue crack growth predictions under *VA* obtained from even a simple non-interaction model [26] correlates well with experimental data for load variations with small interaction effects and full aircraft spectra with

randomly distributed load cycles. A major followup question is whether a simple interaction model would be sufficient to describe the retardation effects during the large and distinct load sequences occurring in the applied spectrum.

This paper presents the study on the application of a simple interaction model (yield zone: Wheeler), in order to answer the question, whether or not a simple retardation model is sufficient to describe the interaction effects in *FMLs* under *VA* loading.

2 Fibre Metal Laminates

FMLs are built up of alternating metal- and fiber layers. After *ARALL* [1], *GLARE* is the second member of the *FMLs* material family. Unlike *ARALL*, *GLARE* (*GLASS-REINFORCED*) has good fatigue properties in combination with compressive loading [5]. Beside the excellent fatigue characteristics, *GLARE* also has good impact and damage tolerance characteristics [15]. The fiber/epoxy layers act as barriers against corrosion of the inner metallic sheets, whereas the metal layers protect the fiber/epoxy layers from picking up moisture. The laminate has an inherent high burn-through resistance as well as good thermal insulation properties.

For standard *GLARE*, aluminum (alloy) 2024-T3 sheets and S2-glass fibers are bonded together with FM94 epoxy adhesive to form a laminate. This stack is cured in an autoclave at 120 °C and 6 bar for 1½ hour. The fiber orientation is de-

fined with respect to the rolling direction of the aluminum layers and each orientation represents a prepreg layer of 0.133 mm nominal thickness. Detailed description of standard *GLARE* grades are given in [15].

3 Fatigue in *FMLs*

GLARE, being a material made-up of metal and composite, exhibit the properties of both metals and composites. The metallic layers show fatigue crack growth similar to monolithic metals and the composite layers show delamination at the metal-composite interfaces. The fibers in

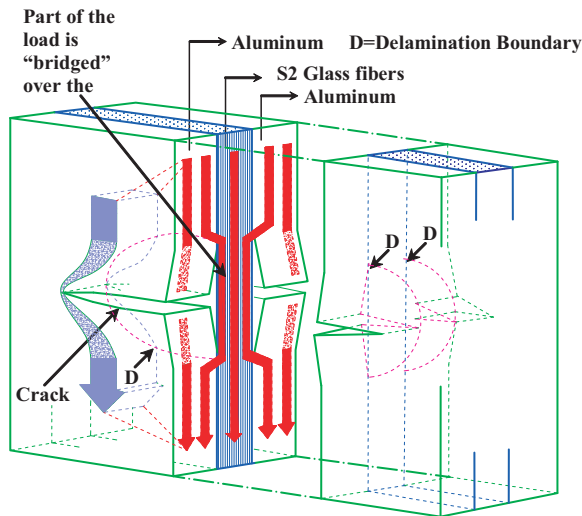


Fig. 1 Crack bridging of the fibers and delamination of the layers

FMLs are insensitive to the fatigue loading, while the metal layers exhibit the crack initiation and propagation. The fibers transfer load over the fatigue crack in the metal layers and restrain the crack opening. This phenomenon is called fiber bridging (Figure 1). An other phenomenon illustrated in Figure 1 is the delamination at the metal-fiber interface in the wake of the crack. The cyclic shear stresses at the interface as result of the load transfer from the metal to the fiber layers induce delamination growth. Both the fatigue crack growth in the metal layers and the delamination growth at the interfaces form a balanced

and so called coupled process.

4 Selective variable amplitude

A selective variable amplitude load spectrum is defined as a constant amplitude spectrum with few load variations such as single overload/underload, multiple overload/underload and their combinations in different sequences. These selective load variations are the building blocks of the (aircraft) service spectrum[27]. In the research presented here, the selective variable amplitude spectrum has been utilized to get the basic understanding of crack growth behavior of *FMLs* under aircraft spectra.

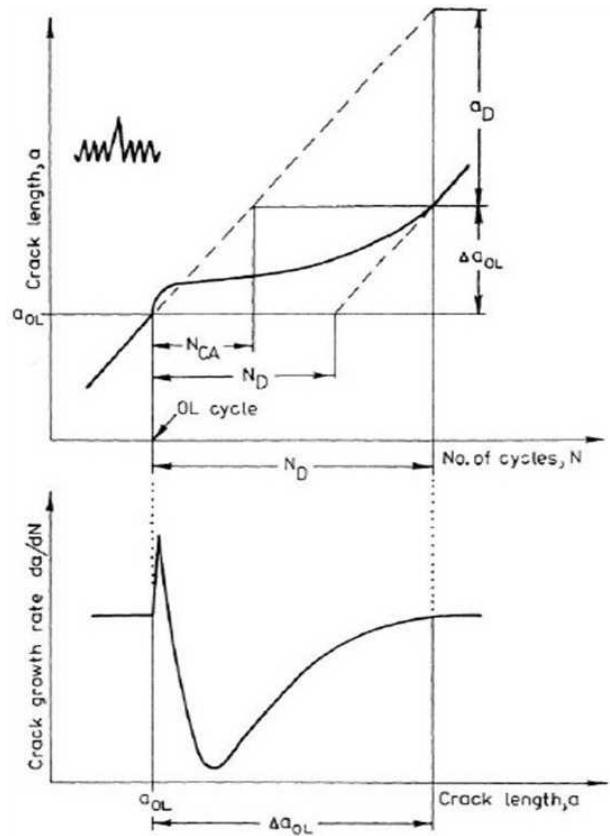


Fig. 2 Schematic of crack growth retardation following an overload in metals [28]

Application of overloads in the *CA* baseline cycles causes a load interaction effect detailed schematically in figure 2. This entire mechanism is known as (delayed) retardation of crack

growth. The magnitude and extent of the retardation is measured by the parameters defined in figure 2, i.e. the number of delay cycles N_D , the delay distance a_D and the overload-effected crack growth increment Δa_{OL} . Similar results and phenomena are present in case of multiple overloads. In case of single/multiple overloads the main parameter influencing crack growth retardation is the overload ratio ($R_{OL} = S_{OL}/S_{max}$). Thus, increase in R_{OL} will result in an increase in N_D , a_D and Δa_{OL} , and a reduction in the da/dN level.

5 Yield zone model

According to Gallagher [29] and Schijve [30], the models that try to explain the interaction effect by considering the condition in front of crack tip (plastic zone) are labelled as Yield Zone Models. Wheeler [31] started this generation of prediction models involving interaction effects in the prediction of crack growth.

The Wheeler [31] prediction model is based on the damage accumulation relation but modified by a simple retardation parameter C_P (equation (1)).

$$a = a_0 + \sum_{i=1}^n C_P f(\Delta K, r_i, \dots) \quad (1)$$

where C_P varies from 0 to 1 depending on the location of the crack tip in a previously created larger zone (r_P in figure 3) and the plastic zone size of the current load cycle r_i . With $r_p = (a_{OL} + r_{OL}) - a_i$ the C_P is calculated using:

$$C_P = \begin{cases} \left[\frac{r_i}{r_P} \right]^m & \text{when } r_i < r_P \\ 1 & \text{when } r_i \geq r_P \end{cases}$$

or

where r_i is the current plastic zone size, r_{OL} is the overload plastic zone size, a_{OL} is the crack length at overloading illustrated in figure 3. m is the experimentally calculated exponent which depends on the stress level, the crack shape as well as the load spectrum. Wheeler used Irwin plane stress relation [32] for the plastic zone size computation. Wheeler assumed that m once calibrated can be used for other spectra. But later it was shown that the accuracy of predictions will

suffer if different loading spectra are used with the same m value [33, 34]. For the metallic structures the Wheeler model is unable to predict the phenomenon of crack arrest after a high overload, because the predicted retardation factor immediately after the overload will not be zero [35]. Secondly, the Wheeler model did not recognize the occurrence of delayed retardation. Actually, the model assumes very simple crack growth behavior; whereas immediately after application of peak loads the phenomenon is very complex.

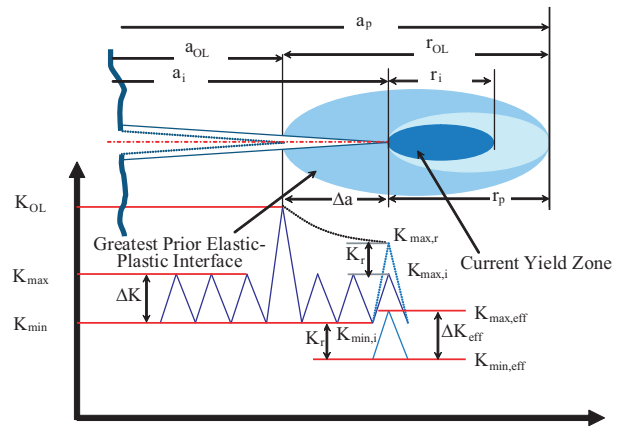


Fig. 3 Relative sizes of plastic zones in the yield zone models. [36]

6 Analytical prediction model

A model has been developed based on understanding so far of fatigue crack growth in FMLs under VA loading. This model is also used for the validation of current hypothesis of small and predictable crack growth retardation. The LDA model of Khan et. al. [26] has been used as the basis for development of this VA prediction model using Wheeler yield zone model adapted for FMLs. The flow diagram of this yield zone prediction model is shown in figure 4.

The original analytical model [22, 25] describes the bridging stress, the delamination shape extension, the stress intensity factor and the crack growth. It can easily be concluded from this model that the bridging stress, the crack opening contour and the delamination shape are in balance with each other. The bridging stress is

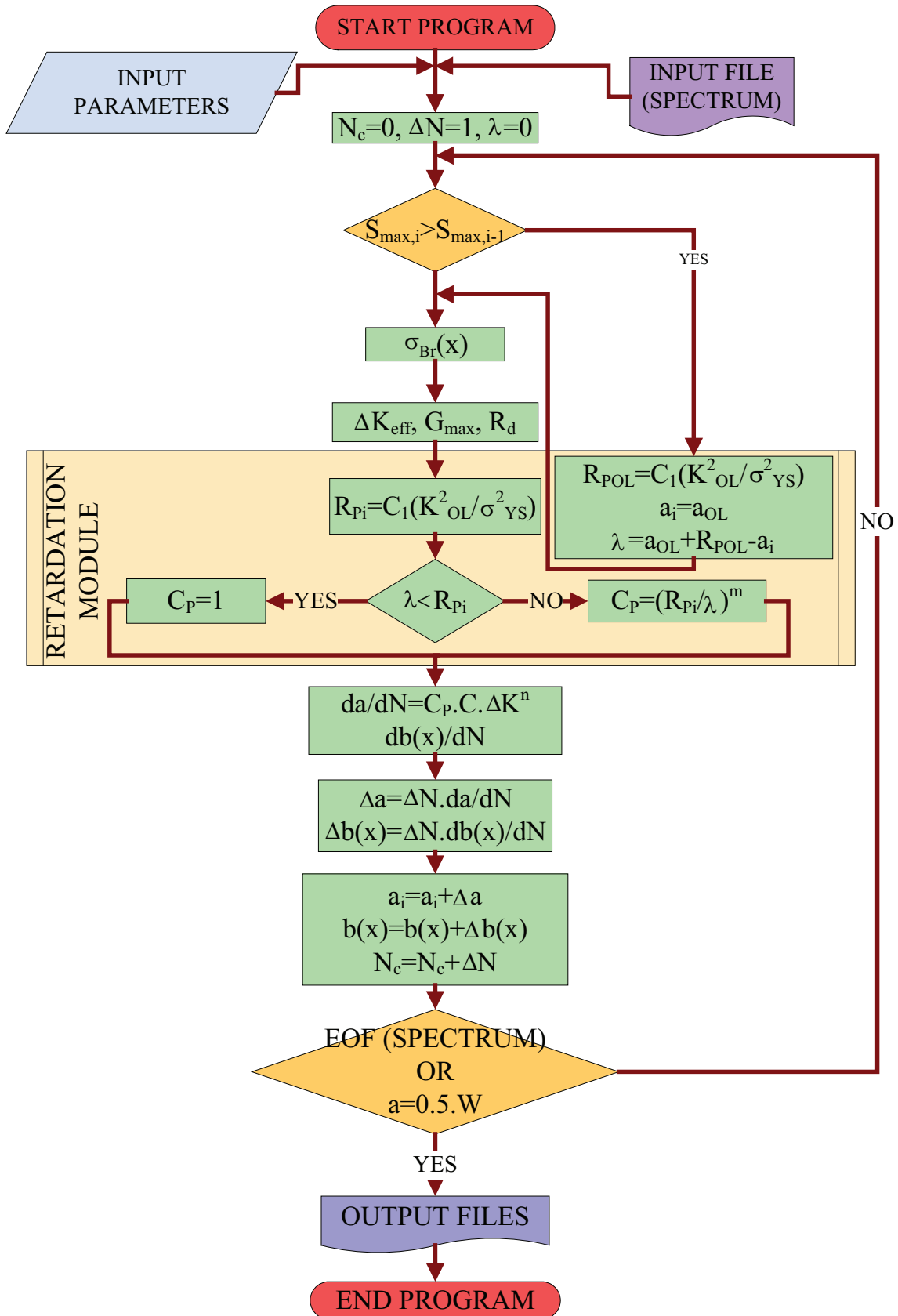


Fig. 4 Flow diagram for the crack growth prediction model

FATIGUE CRACK GROWTH PREDICTION OF FIBRE REINFORCED METAL LAMINATES UNDER VARIABLE AMPLITUDE LOADING

obtained by balancing the relations for the crack opening in the metal layers and the elongation and deformation of the fiber layers. Since the fiber layers in *FMLs* bridge most of the load around the crack in the metal layers, the fiber bridging stress has a direct influence on the stress intensity factor at the crack-tip. However, the bridging stress is influenced by the shape of the delamination, which has a significant influence on the crack growth. Delamination growth is described using Paris type relation with two experimentally determined constants C_d , n_d and the energy release rate G [23].

$$\frac{db}{dN} = C_d(\sqrt{G_{d,max}} - \sqrt{G_{d,min}})^{n_d} \quad (2)$$

In the theoretical model, the effective stress intensity factor in *GLARE* is defined as the difference between the far-field stress intensity factor and the bridging stress intensity factor.

$$K_{tip} = K_{farfield} - K_{bridging} \quad (3)$$

Plokker [37] refined the effective stress intensity factor relation using the Schijve [38] correction which is further improved by Rensma [39].

$$\Delta K_{eff} = (0.55 + 0.33R_{K_{tip}} + 0.12R_{K_{tip}}^2)\Delta K_{tip} \quad (4)$$

Where, according to Rensma $R_{K_{tip}} = K_{tip_{min}}/K_{tip_{max}}$.

Finally, the crack growth rate can be determined using the material constants C_{cg} and n_{cg} for the Paris- ΔK_{eff} region and the effective stress intensity range.

$$\frac{da}{dN} = C_{cg}\Delta K_{eff}^{n_{cg}} \quad (5)$$

In order to formulate this analytical approach, a program has been written using the Matlab software. The program starts with defining input variables concerning material parameters, crack geometry and Paris constants for crack propagation and delamination growth. Other important input parameters are the spectrum file, initial delamination shape and loading cycle counter. To make this model functional for all sort of variable

load spectra, an input file system is programmed. The spectrum file consists of stress values listed in the order of applied sequence.

7 Model validation using test data

To validate the model, fatigue crack growth experiments on *GLARE 3-4/3-0.3* with cross-ply fiber orientation have been performed. These fatigue crack growth tests have been performed on center-cracked tension (*CCT*) specimens, for which the geometry is illustrated in figure 5. The starter notches are made by drilling a hole of 3 mm diameter with two saw cuts, directing perpendicular to the loading direction. The total length of the starter notch ($2a_0$) is approximately 5 mm. Load variations are applied on a *CA* base-

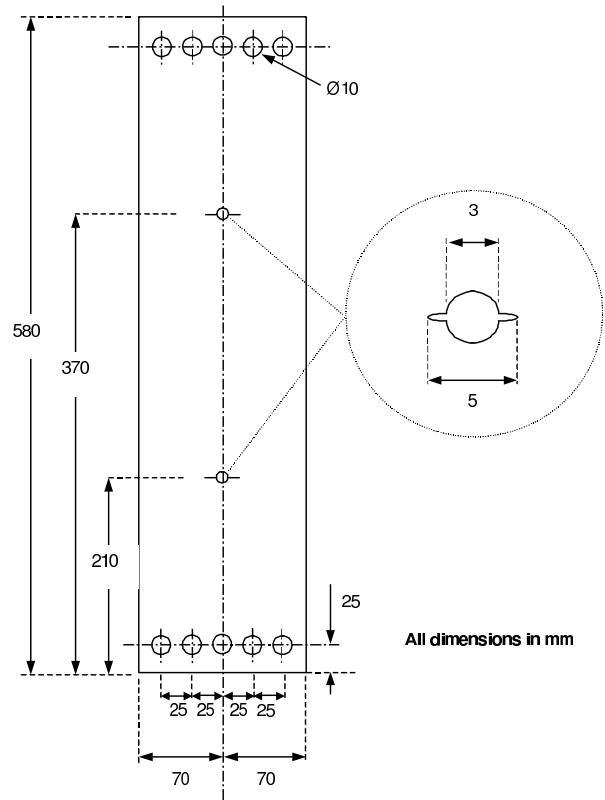


Fig. 5 Centered-cracked Specimen geometry

line spectrum with a maximum stress $S_{max} = 120$ MPa and a stress ratio $R = 0.1$. The single overload spectrum has an overload $S_{OL} = 175$ MPa at 100 kcycles. The multiple overload spectrum has three overloads i.e. $S_{OL1} = 175$ MPa; $S_{OL2} = 158$ MPa and $S_{OL3} = 139$ MPa at 100, 160 and

220 kcycles respectively. Block loading spectra consist of two stress levels $S_{max1} = 100$ MPa and $S_{max2} = 140$ MPa and vice versa with stress ratio $R = 0.1$. Apart from these selective VA loading spectra, representative complex flight spectra are also used for the model validation.

8 Results and discussion

The comparisons of yield zone model predictions with the tests results are shown in figures 6-12. Figure 6 shows the comparison for single overload of 175 MPa in the CA baseline cycles of $S_{max} = 120$ MPa and stress ratio $R = 0.1$.

The yield zone model is able to predict the crack growth retardation in agreement with the experimental data. An interesting observation from figure 6 is that there is hardly any difference between the prediction and experimental data after the application of overload. In other words, the number of delay cycles are almost equal which indicates that it is only the plastic zone that cause the retardation. This can be attributed to the existence of intact fibers which restrain the crack opening leading to the small plastic zone formation. The crack growth rate gets back to the prior level as soon as the crack tip is out of the plastic zone formed by the overload.

Similar to the single overload case (figure 6), the crack growth rate in the multiple overload case (figure 7) gets back to original level depending on the magnitude of S_{OL} and R_{OL} . Figure 7 shows the comparison for the case with multiple overloads of 175, 158 and 139 MPa respectively in the CA baseline cycles of $S_{max}=120$ MPa and $R = 0.1$. It is known from the literature that in metals the retardation region is highly influenced by the magnitude of S_{OL} , and similar behavior is seen in case of *FMLs*. By reducing the S_{OL} from 175 to 158 and then to 139 MPa the crack growth retardation decreases (figure 7).

Figures 8 and 9 show the comparison between yield zone model prediction and test results for the two different sequences of block loads. The stress values are $S_{max1}=100$ MPa, $R = 0.1$ and $S_{max2}=140$ MPa, $R = 0.1$. Figure 8 shows the comparison for the Low-High

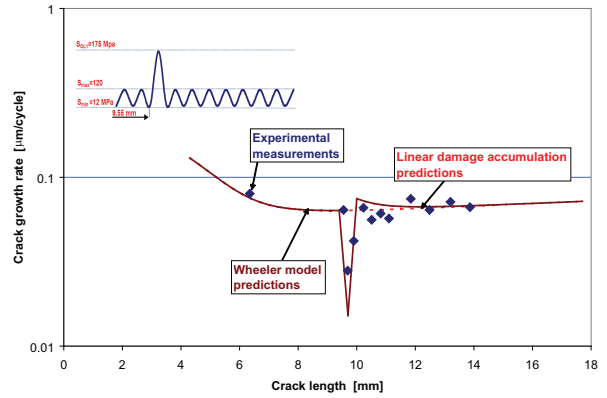


Fig. 6 Correlation between experimental and yield zone model prediction for an overload in a CA baseline test.

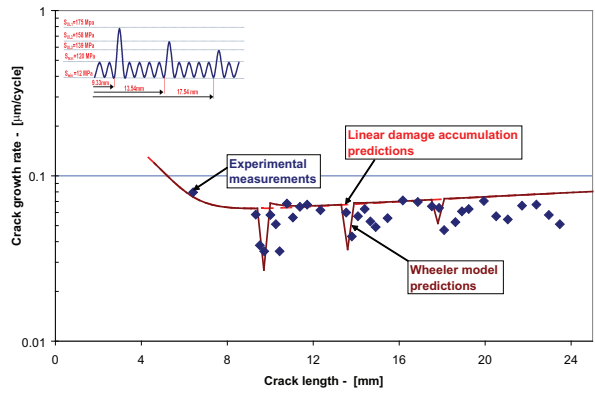


Fig. 7 Correlation between experimental and yield zone model prediction for multiple overloads in a CA baseline test

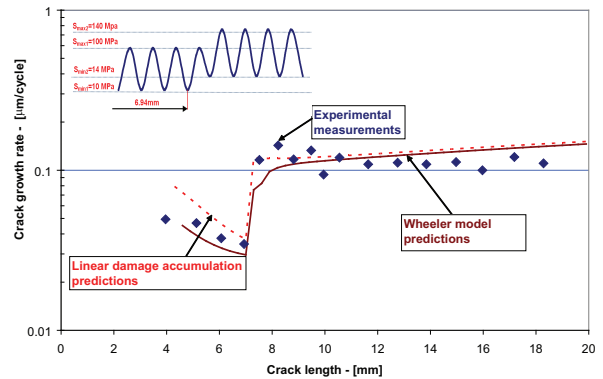


Fig. 8 Correlation between experimental and yield zone model prediction for low-high stress level block loading test.

FATIGUE CRACK GROWTH PREDICTION OF FIBRE REINFORCED METAL LAMINATES UNDER VARIABLE AMPLITUDE LOADING

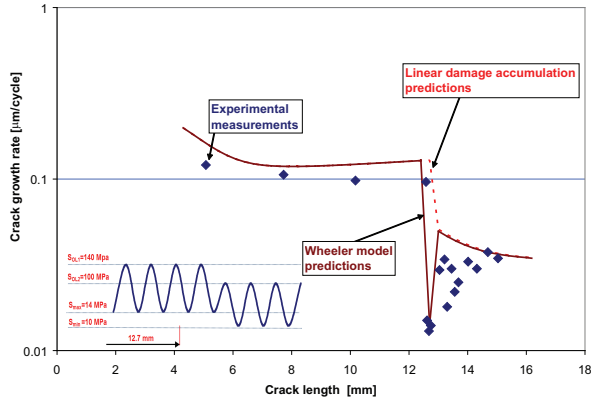


Fig. 9 Correlation between experimental and yield zone model prediction for high-low stress level block loading test.

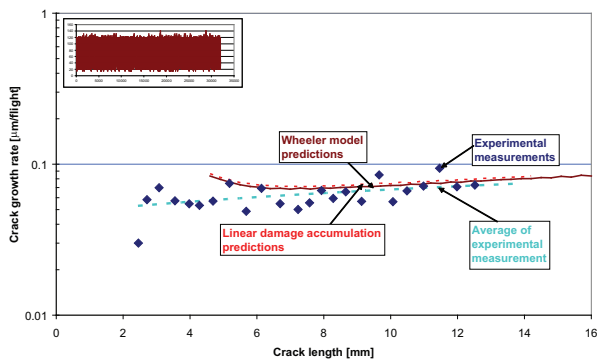


Fig. 10 Correlation between experimental and yield zone model prediction for spectrum I.

block loading case. Since the loading sequence is going from low to high values, there will not be any retardation but due to increase in stress level, crack growth acceleration is observed. The error in this case is less than the cases shown in figures 6 and 7, because the interaction effects are absent in the test.

Figure 9 shows the comparison between test results and the yield zone model predictions in case of the High-Low block loading sequence. The retardation level is computed by the yield zone model but the delay retardation can be observed in the experimental measurements, which is not present in yield zone model predictions. Similar to metals, in *FMLs* a large block of overload cycles creates larger plastic zones resulting in large retardation and related phenomena.

Figures 10-12 exhibit the comparison of crack growth test results with the yield zone

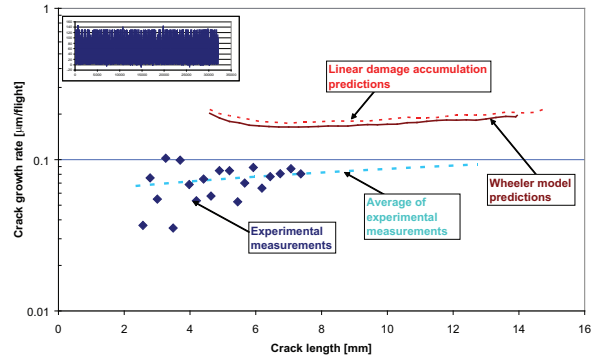


Fig. 11 Correlation between experimental and yield zone model prediction for spectrum II.

model predictions for representative complex aircraft spectra. Three different spectra are used with different S_{max} values and sequences. The loading spectrum used in figure 11 is a severe spectrum with a lot of variations in the stress peaks. The observed mismatch in yield zone model prediction and test result for spectrum II (figure 11), while only a small error is observed for the other two spectra (figures 10, 12) can be attributed to the nature of these spectra. To avoid disclosing proprietary information, only the graphical representation of the three spectra in figures 10- 12 will be used for comparison and discussion. Comparing the spectra, one can observe that spectrum I and II have all loads randomly distributed between minimum and maximum values. Only spectrum III seems to have less amplitude cycles on the lower stress range, but that has no significant effect on crack growth, resulting in similar behavior as spectrum I. However, spectrum II has clearly large load cycles distributed throughout the spectrum with most of the stress cycles in the lower stress range. Comparing to a single overload situation figure 6, the crack in figure 11 seems unable to grow out of the retardation zone of previous high load in the spectrum II before facing subsequent high load. This continuous retardation, not captured by yield zone model, results in the systematic mismatch. This concept is illustrated in figure 13. In case of Wheeler predictions, the crack growth rate returns to the original (prior overload) rate very quickly, while in reality it takes longer (larger number of delay cycles). Secondly,

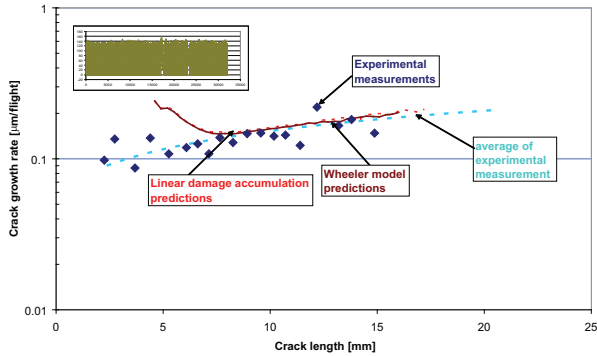


Fig. 12 Correlation between experimental and yield zone model prediction for spectrum III.

in case of complex spectrum like Spectrum II, the situation gets more complex by the application of additional overload while the actual crack growth rate has not reached to the original level. A small error is generated due to the difference of application point (crack growth rate) of overload. This small error is compounded due to the application of consecutive overloads. Because of this, a lower crack growth rate is observed in experiments compared to the predictions (figure 11).

The comparison of the spectrum I and spectrum III are shown in figures 10, 12. The comparison of test results with the yield zone model predictions for the spectrum I and III show very small error. But for the spectrum II (figure 11) the yield zone model predictions are quite far from the test results. The difference lies in the spectrum itself, because if we compare all the three spectra we come to know about the number of overload cycles in spectrum II are more than in spectrum I and III. In the yield zone model and experimental results, it is obvious from all the plots (figures 6- 9) that da/dN gets back to the original level as soon as the retardation effects are over. While in case of spectrum II it looks like the crack tip is trapped in frequently occurring overloads and plastic zones. We can also relate this behavior to de Koning's [40] primary and secondary plastic zone concept that makes the large difference between the prediction and test results.

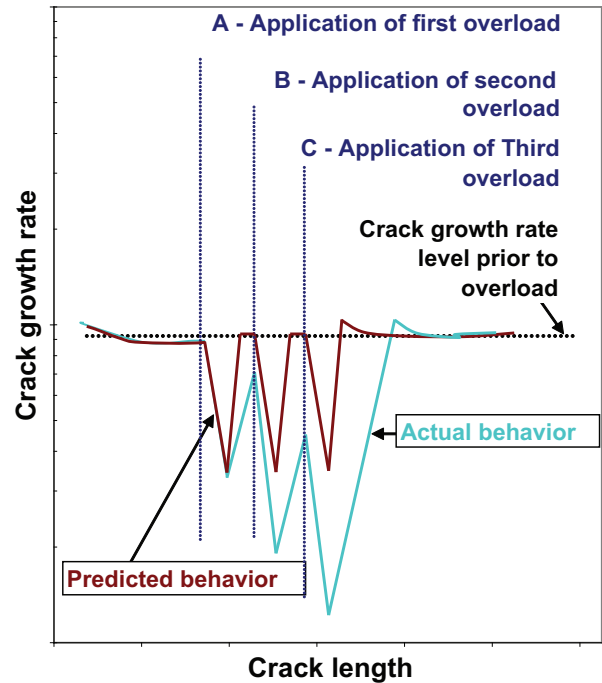


Fig. 13 Schematic of comparison: Actual and predicted fatigue crack growth under complex spectrum loading.

9 Conclusions

The fatigue crack growth behavior in *FMLs* has been investigated using a simple interaction model. The experimental data for different selective and variable amplitude loading spectra reasonably correlates with the yield zone model predictions. The basic assumption of small interaction effects due to crack bridging proves to be valid. However, still some physical phenomena like delay retardation have to be investigated.

References

- [1] Marissen, R., *Fatigue crack growth in ARALL, a hybrid aluminium-aramid composite material, crack growth mechanisms and quantitative predictions of the crack growth rate*, Ph.D. thesis, Delft University of Technology, Delft, 1988.
- [2] Yeh, J. R., "Fracture Mechanics of delamination in Arall laminates," *Engineering Fracture Mechanics*, Vol. 30, 1988, pp. 827–837.
- [3] Macheret, J., Teply, J. L., and Winter, E. F. M., "Delamination shape effects in aramid-epoxy-aluminum (ARALL) laminates with fatigue cracks," *Polymers & Composites*, Vol. 10, 1989, pp. 322–327.

FATIGUE CRACK GROWTH PREDICTION OF FIBRE REINFORCED METAL LAMINATES UNDER VARIABLE AMPLITUDE LOADING

- [4] Ritchie, R., Weikang, Y., and Bucci, R. J., "Fatigue crack propagation in Arall laminates: measurement of the effect of crack-tip shielding from crack bridging," *Engineering Fracture Mechanics*, Vol. 32, 1989, pp. 361–377.
- [5] Roebroeks, G. H. J. J., *Towards Glare, The development of a fatigue insensitive and damage tolerant aircraft material*, Ph.D. thesis, Delft University of Technology, Delft, 1991.
- [6] Macheret, Y., Bucci, R. J., Nordmark, G. E., and Kipp, T. R., "Failure analysis of aramid fiber reinforced aluminum laminates with surface and through thickness fatigue cracks," *ASTM Special Technical Publication*, Vol. 1203, 1993, pp. 171–87.
- [7] Lin, C. T. and Kao, P. W., "Effect of fiber bridging on the fatigue crack propagation in carbon fiber-reinforced aluminium laminates," *Material Science Engineering*, Vol. A190, 1995, pp. 65–73.
- [8] Toi, R., "An empirical crack growth model for fiber/metal laminates." *18th symposium of the international committee on aeronautical fatigue, Melbourne, Australia*, 1995, pp. 899–909.
- [9] Yeh, J. R., "Fatigue crack growth in fiber-metal laminates," *International Journal of Solids Structures*, Vol. 32, 1995, pp. 2063–2075.
- [10] Guo, Y. J. and Wu, X. R., "A theoretical model for predicting fatigue crack growth rates in fibre-reinforced Metal Laminates," *Fatigue Fracture Engineering Materials & Structures*, Vol. 21, 1998, pp. 1133–1145.
- [11] Guo, Y. and Wu, X., "A phenomenological model for predicting crack growth in fiber-reinforced metal laminates under constant-amplitude loading," *Composite Science and Technology*, Vol. 59, 1999, pp. 1825–1831.
- [12] Guo, Y. J. and Wu, X. R., "Bridging stress distribution in center-cracked fiber reinforced metal laminates: modelling and experiment," *Engineering Fracture Mechanics*, Vol. 63, 1999, pp. 147–163.
- [13] Takamatsu, T., Matsumura, T., Ogura, N., Shimokawa, T., and Kakuta, Y., "Fatigue crack growth properties of a GLARE3-5/4 fiber/metal laminate," *Engineering Fracture Mechanics*, Vol. 63, 1999, pp. 253–272.
- [14] Vlot, A., Vogelesang, L. B., and Vries, T. F., "Toward application of fibre metal laminates in large aircraft," *Aircraft Engineering & Aerospace Technology*, Vol. 71, 1999, pp. 558–570.
- [15] Vlot, A. and Gunnink, J. W., *Fibre Metal Laminates- An introduction*, Kluwer Academic Publishers, Dordrecht, The Netherlands, 2001.
- [16] Wu, X. J., "A higher-order theory for fiber-metal laminates," *23rd international congress on aeronautical sciences, Toronto, Canada*, 2002.
- [17] Alderliesten, R. C., Hagenbeek, M., Homan, J. J., Hooijmeijer, P. A., De Vries, T. J., and Vermeeren, C. A. J. R., "Fatigue and damage tolerance of glare," *Applied Composite Materials*, Vol. 10, 2003, pp. 223–242.
- [18] Shim, D. J., Alderliesten, R. C., Spearing, S. M., and Burianek, D. A., "Fatigue crack growth prediction in GLARE hybrid laminates," *Composite Science and Technology*, Vol. 63, 2003, pp. 1759–1767.
- [19] Takamatsu, T., Shimokawa, T., Matsumura, T., Miyoshi, Y., and Tanabe, Y., "Evaluation of fatigue crack growth behaviour of GLARE3 fiber/metal laminates using compliance method," *Engineering Fracture Mechanics*, Vol. 70, 2003, pp. 2603–2616.
- [20] Beumler, T., *Flying Glare - A contribution to aircraft certification issues on strengths properties in non-damaged and fatigue damaged GLARE structures*, Ph.D. thesis, Delft University of Technology, Delft, 2004.
- [21] Suiker, A. S. J. and Fleck, N. A., "Crack tunnelling and plane-strain delamination in layered solids," *International Journal of Fracture*, Vol. 1, 2004, pp. 1–32.
- [22] Alderliesten, R. C., *Fatigue crack propagation and delamination growth in Glare*, Ph.D. thesis, Delft University of Technology, Delft, 2005.
- [23] Alderliesten, R. C., Schijve, J., and van der Zwaag, S., "Application of the energy release rate approach for delamination growth in Glare," *Engineering Fracture Mechanics*, Vol. 73, 2006, pp. 697–709.
- [24] Alderliesten, R. C., "On the available relevant approaches for fatigue crack propagation prediction in Glare," *International Journal of Fatigue*, Vol. 29, 2007, pp. 289–304.
- [25] Alderliesten, R. C., "Analytical prediction model for fatigue crack propagation and delamination growth in Glare," *International Journal of Fatigue*, Vol. 29, 2007, pp. 628–646.
- [26] Khan, S. U., Alderliesten, R. C., and Benedictus, R., "LDA's Applicability for Predicting Fatigue Crack Growth in FML's Under VA Loading," *49th*

AIAA/ASME/ASCE/AHS/ASC Structures, Structural Dynamics, and Materials Conference, Schaumburg, IL., No. AIAA-2008-2017 in AIAA, April 7-10 2008.

- [27] Schijve, J., “Prediction of fatigue crack growth in 2024-T3 alclad sheet specimen under flight-simulation loading,” Tech. rep., Delft University of Technology, Delft, LR-574, 1981.
- [28] Skorupa, M., “Load interaction effects during fatigue crack growth under variable amplitude loading-A literature review. Part I: Empirical trends,” *Fatigue & Fracture of Engineering Materials and Structures*, Vol. 21, 1998, pp. 987–1006.
- [29] Gallagher, J. P., “A Generalized Development of Yield Zone Models,” Tech. rep., AFFDL-TM-74-28-FBR, 1974.
- [30] Schijve, J., *Fatigue of Structures and Materials*, Kluwer, 2001.
- [31] Wheeler, O., “Spectrum loading and crack growth.” Tech. rep., ASMR 72 MetX also G.D. Report FZM 5602, 1970.
- [32] Irwin, G. R., “Linear fracture mechanics, fracture transition, and fracture control,” *Engineering Fracture Mechanics*, Vol. 1, 1968, pp. 241–257.
- [33] Finney, M., “Sensitivity of fatigue crack growth prediction (using Wheeler retardation) to data representation,” *Journal of Testing and Evaluation*, Vol. 17, 1989, pp. 74–81.
- [34] Meggiolaro, M. A. and Pinho de Castro, J. T., “Comparison of load interaction models in fatigue crack propagation,” *16th Brazilian congress of Mechanical Engineering*, 2001.
- [35] Corlby, D. M. and Packman, P. F., “On the Influence of Single and Multiple Peak Overloads on Fatigue Crack Propagation in 7075-T6511 Aluminum,” *Engineering Fracture Mechanics*, Vol. 5, 1973, pp. 479–497.
- [36] Khan, S. U., Alderliesten, R. C., Schijve, J., and Benedictus, R., “On the fatigue crack growth prediction under variable amplitude loading,” *Computational and experimental analysis of damaged materials 2007*, edited by D. G. Pavlou, Transworld Research Network, Kerala, India., 2007.
- [37] Plokker, H. M., Alderliesten, R. C., and Benedictus, R., “Crack Closure in fiber metal Laminates,” *Fatigue and Fracture of Engineering Materials and Structures*, Vol. 30, 2007, pp. 608–620.

[38] Schijve, J., “Some formulas for the crack opening stress level,” *Engineering Fracture Mechanics*, Vol. 14, 1981, pp. 461–465.

[39] Rensma, E., *Investigation of innovative concepts for hybrid structures.*, Master’s thesis, Delft University of Technology, Delft., 2007.

[40] de Koning, A. U. and van der Linden, H. H., “Prediction of fatigue crack growth rates under variable amplitude loading using a simple crack closure model,” Tech. Rep. NLR MP 81023U, National Aerospace Laboratory NLR, Amsterdam. The Netherlands, 1981.

Copyright Statement

The authors confirm that they, and/or their company or institution, hold copyright on all of the original material included in their paper. They also confirm they have obtained permission, from the copyright holder of any third party material included in their paper, to publish it as part of their paper. The authors grant full permission for the publication and distribution of their paper as part of the ICAS2008 proceedings or as individual off-prints from the proceedings.